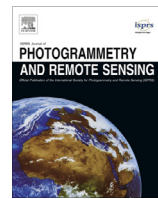


Contents lists available at ScienceDirect

ISPRS Journal of Photogrammetry and Remote Sensing

journal homepage: www.elsevier.com/locate/isprsjprs

Measurement of ground displacement from optical satellite image correlation using the free open-source software MicMac

Ana-Maria Rosu ^{a,*}, Marc Pierrot-Deseilligny ^b, Arthur Delorme ^a, Renaud Binet ^c, Yann Klinger ^a^aLaboratoire de tectonique et mécanique de la lithosphère, Institut de Physique du Globe de Paris, France^bLaboratoire de géomatique appliquée, Ecole Nationale des Sciences Géographiques, Institut National de l'Information Géographique et Forestière, France^cLaboratoire PS/TIS, Centre National d'Etudes Spatiales, France

ARTICLE INFO

Article history:

Received 28 September 2013

Received in revised form 4 March 2014

Accepted 7 March 2014

Available online xxxx

Keywords:

Satellite image

Ground displacement

Image correlation

COSI-Corr

Medicis

MicMac

ABSTRACT

Image correlation is one of the most efficient techniques to determine horizontal ground displacements due to earthquakes, landslides, ice flows or sand dune migrations. Analyzing these deformations allows a better understanding of the causes and mechanisms of the events. By using sub-pixel correlation on before- and after-event ortho-images obtained from high resolution satellite images it is possible to compute the displacement field with high planimetric resolution. In this paper, we focus on measuring the ground displacements due to seismotectonic events. The three sub-pixel correlators used are: COSI-Corr – developed by Caltech, a free, closed-source correlator, dependent on commercial software (ENVI) and widely used by the geoscience community for measuring ground displacement; Medicis – developed by CNES, also a closed-source correlator capable of measuring this type of deformation; and MicMac – developed by IGN, the free open-source correlator we study and tune for measuring fine ground displacements. We measured horizontal ground deformation using these three correlators on SPOT images in three study cases: the 2001 Kokoxili earthquake, the 2005 dyke intrusion in the Afar depression and the 2008 Yutian earthquake.

© 2014 International Society for Photogrammetry and Remote Sensing, Inc. (ISPRS) Published by Elsevier B.V. All rights reserved.

1. Introduction

Measuring the fine displacements associated with an earthquake represents a key issue in seismotectonics, offering information about the geometry of the ruptured fault and the energy released by the earthquake (Van Puymbroeck et al., 2000).

The most common method for measuring these displacements is based on field measurements. However, the fault area is often hard to access and complex fault ruptures are not easy to detect in the field; depending on the extent of the fault slip, it can be measured only in a limited number of locations (Leprince et al., 2007a).

Another technique for measuring this type of displacement is by using permanent Global Navigation Satellite System (GNSS) receivers. This technique can only provide sparse coverage and it is impossible to have measurements if the area is not kept under surveillance. As the area of co-seismic ground displacement is *a priori* unknown, it is not always possible to have measurements before the event.

Satellite imagery using synthetic aperture radar (SAR) or optical satellites can overcome some of the limitations of the techniques mentioned before. The satellite images cover a large area – the fault rupture is partially or totally visible.

Compared to the optical sensor, the interferometric SAR technique can be used in all weather and nighttime acquisitions (Massonnet and Feigl, 1998). However this technique is unable to provide displacement maps in the near-field of the fault because the large amplitudes of the displacements present in this area cause the decorrelation of the interferometric phase, so the displacements cannot be estimated. Furthermore, SAR correlation gives low resolution planimetric results, and InSAR provides mainly the near-vertical component.

High-resolution optical satellite imagery provides detailed images of the ground and most importantly, it can resolve the near-fault displacement (Van Puymbroeck et al., 2000). The displacement field can be measured using the correlation of images acquired before and after the event (therefore the temporal baseline is one of the main issues of the correlation).

Optical satellite imagery has extended archives which allows measurements of old earthquakes and could also provide the before-event images when an earthquake occurs. Unlike with InSAR

* Corresponding author. Address: Laboratoire de tectonique et mécanique de la lithosphère, Institut de Physique du Globe de Paris, 75238 Paris cedex 05, France. Tel.: +33 678062697.

E-mail address: am.rosu@laposte.net (A.-M. Rosu).

data, the combination of different archives is possible (Hollingsworth et al., 2012) and is a major advantage of using optical satellite images.

Numerous studies on sub-pixel correlation applied to high-resolution satellite images such as SPOT have shown the efficiency of this technique for measuring ground displacements due to earthquakes (Michel and Avouac, 2002; Dominguez et al., 2003; Binet and Bollinger, 2005; Klinger et al., 2006; Leprince et al., 2007b), landslides (Delacourt et al., 2004; Casson et al., 2005), ice flows (Scambos et al., 1992) and sand dune migrations (Hermas et al., 2012). Analyzing these deformations allows a better understanding of what triggered the event (e.g. analyzing the faults and the displacement field caused by an earthquake can supply extremely important information about the seismic mechanisms).

Sub-pixel detection capability is required in order to measure the displacements which are generally smaller than the image pixel size. In theory, the sub-pixel correlation method using a pair of SPOT panchromatic images could provide fault slip measurements with an accuracy of 0.1 px (Michel and Avouac, 2002; Dominguez

et al., 2003). Therefore, using images with a ground pixel size of 2.5–10 m, the smallest displacements that may be measured are 0.25–1 m. However, the sub-pixel detection is highly dependent on the quality and the noise level of the data. Important matters to take into account when doing correlation are the texture of the images and factors causing great changes in aspect between the two images due to diachronism (the period of time between the two image acquisitions). Seasonal variations could generate changes in the landscape, which might cause decorrelation. In order to avoid parallax problems due to digital elevation model imprecision, it is preferable to use satellite images acquired with very similar incidence angles, close to nadir.

The purpose of this article is to present free open-source software, MicMac, capable of measuring the two-dimensional displacements by optical image correlation and free from most of the drawbacks of the correlators used up until now (e.g. not open-source and hence not easily adaptable to specific cases, lack of robustness in cases where the time interval between the two image acquisitions is very significant or dependent on commercial softwares). In this paper we present the sub-pixel correlation results obtained with MicMac, compared with those obtained using two other correlators, COSI-Corr and Medicis, both of which are used by the geoscience community. The horizontal displacements induced by seismotectonic events were measured using pre-event and post-event SPOT ortho-images. The three study cases are the Kokoxili earthquake ($M_w \sim 7.8$, November 2001, Tibetan Plateau), the September 2005 rifting event of Afar (Ethiopia) and the Yutian earthquake ($M_w \sim 7.1$, March 2008, Tibetan Plateau).

2. Methodology

2.1. Image correlation

The basic parameters of the correlation are the “sliding window”, the “search space” (the correlator computes a correlation score for every position given by the “discretization step” in the search space and keeps the best one; the discretization step defines the sub-pixel precision of the correlation results) and the “step” (distance in pixels between two consecutive parallax estimations, defining the correlation image size). The spatial resolution of the displacement is directly related to the size of the correlation window. The use of a small correlation window implies a result with a higher spatial resolution, which is extremely important if a fine description of the near-fault area is desired. However, the noise

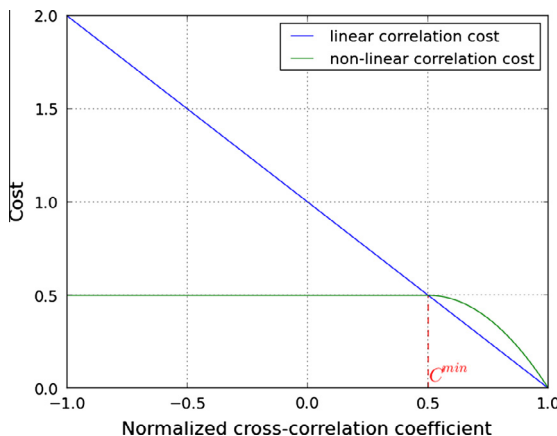


Fig. 1. Linear and non-linear correlation cost in MicMac. By default the correlation cost is linear ($\text{Cost} = 1 - \text{Cor}$, where Cor is the normalized cross-correlation coefficient). When dealing with images with great inhomogeneity, a non-linear cost is used in order to limit the impact of the noisy signal on the whole measurement: $\text{Cost} = \left(1 - \left(\frac{\text{Max}(\text{Cor}, C^{\min}) - C^{\min}}{1 - C^{\min}}\right)^{\gamma}\right) * (1 - C^{\min})$, where C^{\min} is the correlation threshold (below this value, the correlation has no influence) and γ determines the influence of the correlation scores (in our studies, $C^{\min} = 0.5$, $\gamma = 2$).

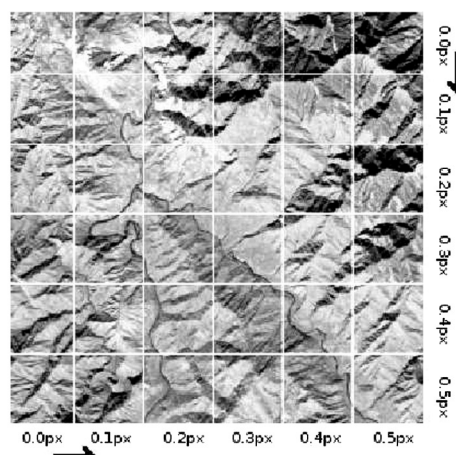


Fig. 2. Synthetic displacement field to retrieve by correlation: the slave image was created using the reference image, a QuickBird satellite image, by dividing it into blocks and moving them along columns and lines, creating successive offsets of 0.1 px per block. The synthetic offsets values go from 0 px to 0.5 px. The correlation results obtained using COSI-Corr, Medicis and MicMac are in Figs. 3 and 4.

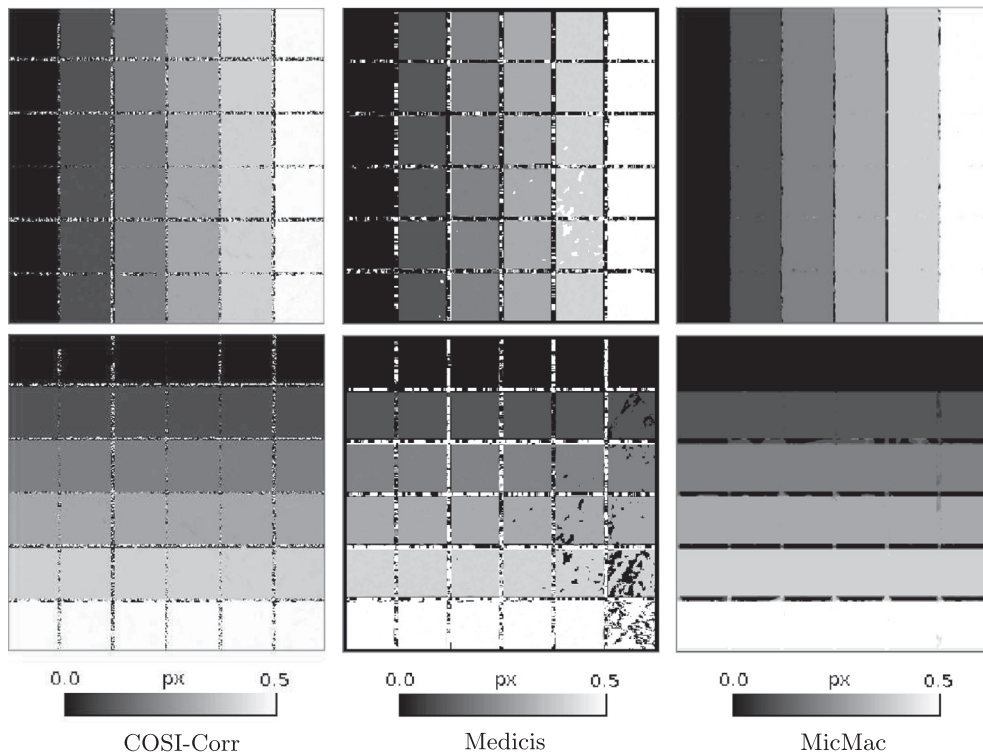


Fig. 3. The two disparity maps, in columns and lines, obtained with COSI-Corr, Medicis and MicMac on the images from Fig. 2. The sizes of the correlation window used are 32×32 px for COSI-Corr, 33×33 px for Medicis and MicMac. The three correlators retrieve well the synthetic deformation field going from 0 to 0.5 px in columns and lines. COSI-Corr's results have very few correlation artifacts, Medicis' results are slightly noisier than COSI-Corr's, and MicMac's results are very close to the theoretical deformation field.

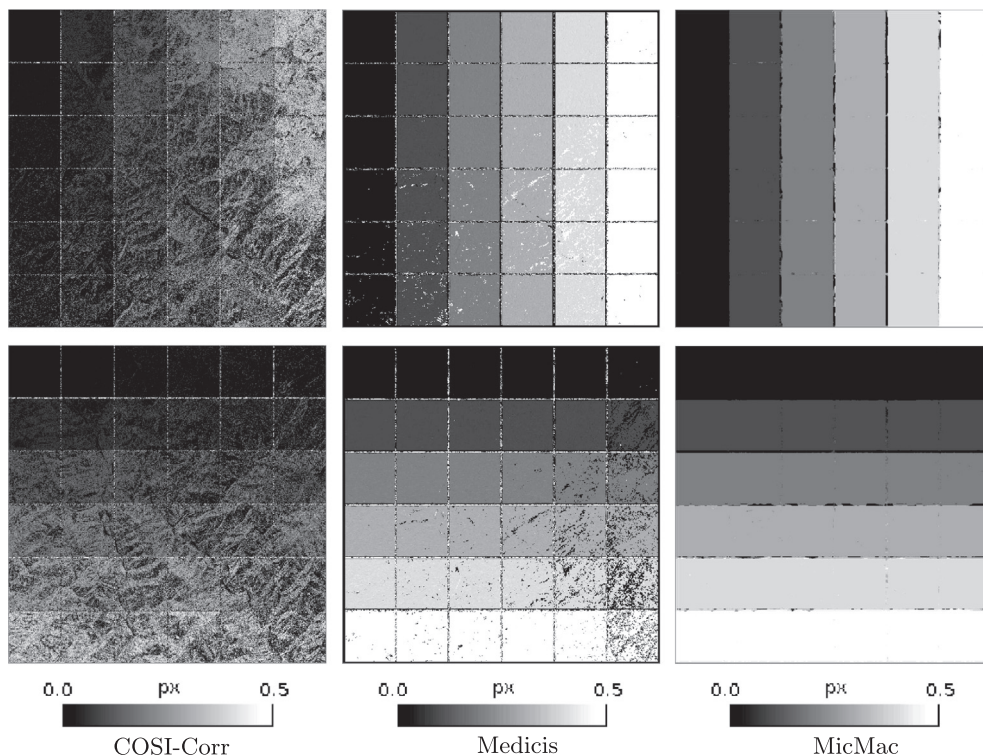


Fig. 4. The two disparity maps, in columns and lines, obtained with COSI-Corr, Medicis and MicMac on the images from Fig. 2. The sizes of the correlation window used are 8×8 px for COSI-Corr, 9×9 px for Medicis and MicMac. COSI-Corr's results are not satisfactory, they are very noisy and the deformation field is not well retrieved. Medicis' results are noisier than the ones obtained using a larger correlation window (Fig. 3), but the deformation field is well retrieved. MicMac's results retrieve very well the synthetic deformation field.

Table 1

Correlation parameters for COSI-Corr, Medicis and MicMac used in all three study cases; the parameters, specific to each correlator, are described in 2.2.1, 2.2.2 and 2.2.3.

Correlators	Parameters	Values
COSI-Corr	Mask threshold	0.9
	Number of iterations	2
Medicis	Initial resemblance threshold	0.6
	Final resemblance threshold	0.8
	Exploration area	7 × 3
	Sub-pixel precision	0.01
MicMac	C^{min}	0.5
	γ	2
	Exploration area	5 × 5
	Number of scanning directions	14
	Regularization term	0.3
	Sub-pixel precision	0.05

increases with the reduction of the window size (Binet and Bollinger, 2005); therefore, this must be seen as a compromise between the required resolution and the noise.

The correlation output consists of two disparity maps with the relative horizontal displacements in rows and in columns plus the correlation scores image which represents the confidence in the correlation for each pixel. When working on georeferenced images, the two disparity maps contain the east-west and north-south components of the displacement.

2.2. Correlators used

Sub-pixel horizontal displacement field is computed using three correlators: COSI-Corr, Medicis and MicMac.

2.2.1. COSI-Corr (Co-Registration of Optically Sensed Images and Correlation)

COSI-Corr is a software module developed using IDL (Interactive Data Language) and integrated with ENVI, implemented at the Caltech Tectonics Observatory (USA). In Ayoub et al. (2009), COSI-Corr is described as providing tools to accurately orthorectify, co-register, and correlate optical remotely sensed images (aerial and pushbroom satellite images) with the ultimate objective of

retrieving ground surface deformation from multi-temporal images. This software is widely used by the geoscience community.

The correlation method implemented in COSI-Corr (described in Leprince et al. (2007b)) is based on frequency-domain correlation. The relative displacement between two patches is estimated from the phase difference of their Fourier transforms. The correlation process consists of two steps. The first step determines the pixelwise displacement between two patches (windows) to correlate. The peak correlation method is used to initialize, and then to iteratively relocate the patches to compensate for their relative displacement. The pixelwise displacement being estimated, a final correlation is operated on relocated patches to determine the subpixel displacement using a minimization algorithm (Van Puymbroeck et al., 2000; Leprince et al., 2007b).

COSI-Corr's graphical user interface gives the user the possibility of choosing the size of the "correlation window", the "step" between two consecutive parallax estimations, "mask threshold" (allows the masking of frequencies according to the amplitude of the log-cross-spectrum for reducing the noise in the measurements; a value close to one is appropriate in most cases (Ayoub et al., 2009)), and the "number of iterations" (two to four iterations are adequate in most cases (Leprince et al., 2007b)). There is an optional resampling step where the patches to correlate are relocated from sinc resampling. This option theoretically eliminates most of the biases at the sub-pixel scale. However, it greatly increases the processing time (on average by a factor of 10) and it is rarely useful on noisy images (Ayoub et al., 2009). After testing this option, we decided not to use it since we did not notice any improvement in the results.

2.2.2. MEDICIS (*Moyen d'Evaluation de Décalages entre Images, Commun à l'Imagerie Spatiale*)

Medicis is developed by CNES (Centre National d'Etudes Spatiales, France). It can be used for sensor calibration, digital elevation model (DEM) and digital surface model (DSM) computation, image overlay and computing deformation between images. Its application stretches to every field where measuring the similarity between pixels is needed, such as remote sensing, geology and medicine.

Medicis offers both a spatial and a frequency correlator. We chose the frequency domain correlator because it has shorter computation time and gives similar results. The computation method is the following: first, the pixelwise disparities in lines and columns

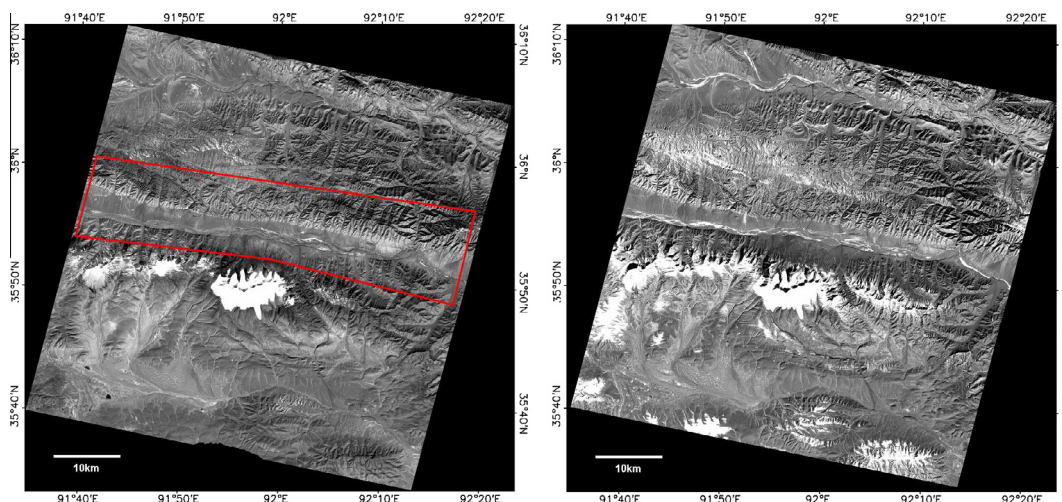


Fig. 5. The pair of ortho-images used for the study of the 2001 Kokoxili earthquake. The pre-event image is from SPOT1 (29 September 1989, incidence angle: L4.60°) and the post-event image is from SPOT4 (30 November 2002, incidence angle: L4.50°). The area where the results are presented (Fig. 6) is marked in red. (For interpretation of the references to color in this figure legend, the reader is referred to the web version of this article.)

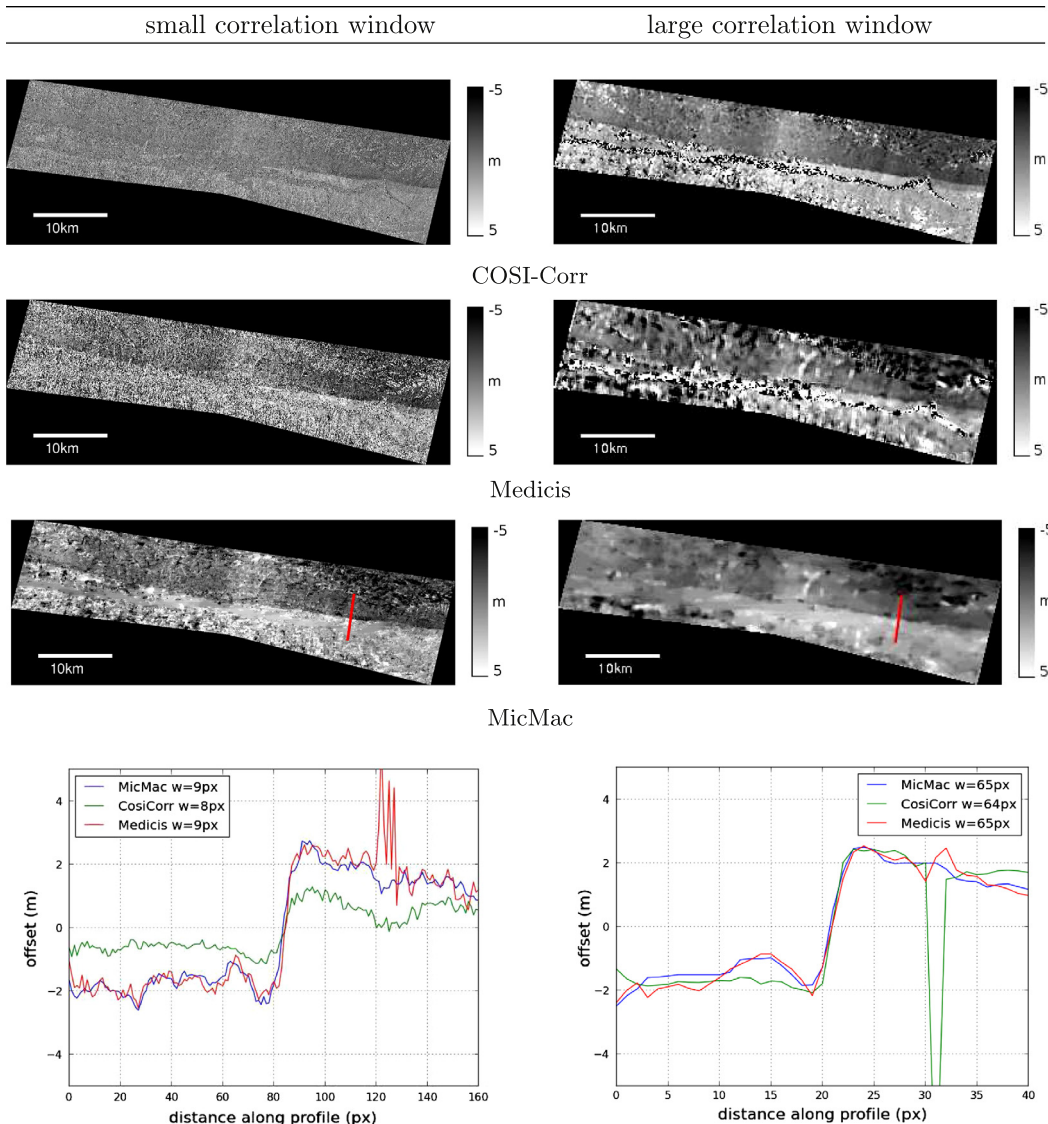


Fig. 6. East-west component of the co-seismic offset field from the 2001 Kokoxili earthquake, using the pair of SPOT ortho-images from Fig. 5. The small correlation windows are 8×8 px (for COSI-Corr) and 9×9 px (for Medicis and MicMac), and the large correlation windows are 64×64 px (for COSI-Corr) and 65×65 px (for Medicis and MicMac). Perpendicular profiles were stacked over a width of approximately 6.5 km and a length of 6.5 km using the weighted median method. For the small correlation window, COSI-Corr underestimates the amplitude of the co-seismic offset; Medicis' result is a bit noisier than MicMac's, but the amplitude of the offset is the same for both, and the same than with the large correlation window. For the large correlation window, all the three correlators retrieve the same amplitude of the offset (~ 4.5 m).

are estimated using the peak correlation method and then the sub-pixel displacement is computed. A “maximum exploration area” (or “search space”) is given around an estimated disparity. An “initial resemblance threshold” defines the lower bound of the correlation coefficient, at pixel level; the sub-pixel disparity is computed only for couples (line, column) with the correlation score above this threshold. Sub-pixel displacements can be measured by applying fractional shifts to the sliding window (Inglada et al., 2007), done by image interpolation. The parameter “precision of localization” manages the fractional shifts and it represents the required sub-pixel precision – the accepted values are between 0 (extremely good precision) and 0.05 (poor). Dichotomy is used for an iterative precise search by resampling using the apodized sinc function. A correlation solution is validated only if its correlation score is above the “final resemblance threshold”. Global shifts between the images are computed by averaging locally measured shifts obtained on all retained sampling points (Bicheron et al., 2011).

2.2.3. MicMac (*Multi Images Correspondances par Méthodes Automatiques de Corrélation*)

MicMac¹ is free open-source software, distributed under the CeCILL-B license, implemented at IGN (Institut National de l'Information Géographique et Forestière, France). It computes multi-image sub-pixel correlation in the spatial domain.

MicMac's fields of application include three-dimensional modeling in archeology, architecture for cultural heritage² and geology and surveying for environmental applications (Guérin et al., 2012; Lisein et al., 2013).

Among the three correlators presented in this paper, MicMac is the only one using regularization. This technique can provide very good results when using small correlation windows, which is well-suited to our purpose of obtaining results with a high spatial

¹ <http://logiciels.ign.fr/?Micmac>.

² <http://www.tapenade.gamsau.archi.fr>.

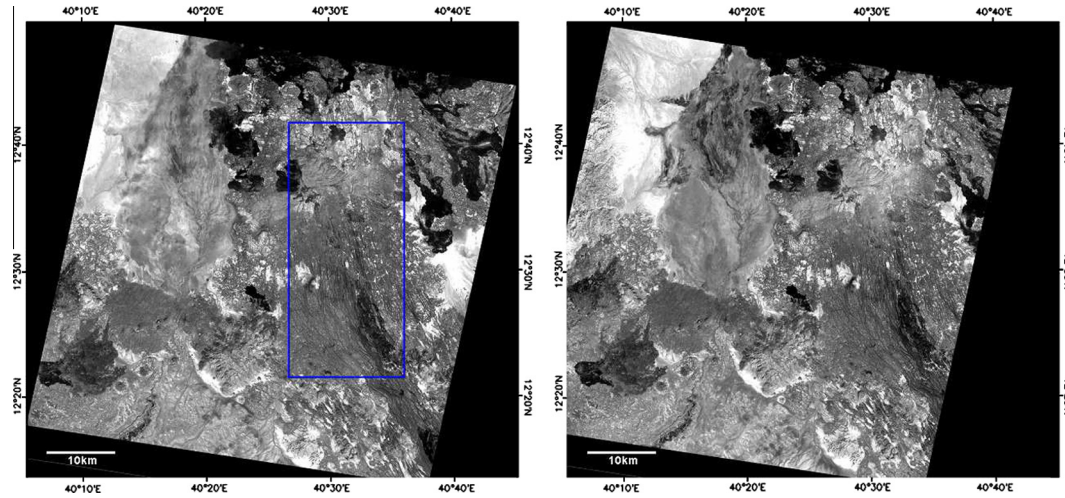


Fig. 7. The pair of ortho-images used for the study of the September 2005 mega-dyke episode in the Afar region. Both the pre-event image (19 December 2004, incidence angle: L0.484217°) and the post-event one (13 January 2006, incidence angle: R0.22152°) are SPOT4 images. The blue box indicates the area where the results are presented in Fig. 8. (For interpretation of the references to color in this figure legend, the reader is referred to the web version of this article.)

resolution in near-fault area. MicMac uses multi-directional dynamic programming when regularizing, with an energy minimization approach based on the “data attachment term” (representing the data consistency) and the “regularization term” (expressing the *a priori* assumption of surface regularity) (Pierrot-Deseilligny and Paparoditis, 2006). A multi-resolution approach consists in starting the computation at a coarse resolution and improving the resolution at each matching level. For MicMac, multi-resolution approach is mainly used in three-dimensional modeling where the combinatorial uncertainty is very high. For two-dimensional correlation, as the initial uncertainty is low, the multi-resolution approach is not used, we work at full resolution at each matching level. The disparity solution is computed in an iterative process, the solution being successively refined at each matching level. Within the “correlation window”, the “search space” (or “exploration area”) is centered on the initial pixel position in the epipolar geometry from the previous correlation level. Within the search space, the correlator computes a disparity for every position defined by the “discretization step” (which controls the sub-pixel precision). An apodized sinc kernel (Thévenaz et al., 2000), obtained by multiplication of the “ideal kernel”, the sinc kernel, by a differentiable and bounded support function, the Hann function, is used for resampling. The disparity with the best similarity/correlation coefficient is the correlation solution.

We adapted MicMac for dealing with the correlation problems that may occur when measuring two-dimensional ground displacements. Among its adjustments, it is important to point out its method of dealing with great spatial inhomogeneities in the resemblance between images with long time baselines (e.g. combination of rocky areas which change very little and snowy areas which completely decorrelate between the two acquisitions). In order to prevent the corruption of measurements in well-correlated areas by poor-correlated ones, MicMac provides the option of using non-linear costs (Pierrot-Deseilligny, 2013) associated with the normalized cross-correlation coefficient (Fig. 1). A correlation threshold, C^{min} , is taken into account, the correlation below this threshold having no influence. Another parameter, γ , controls the influence of correlation scores: the higher the value of γ , the higher the influence of correlation scores close to 1. When *a priori* knowledge of the fault slip direction is available, MicMac offers the possibility of using non-isotropic regularization, where the fault slip direction is taken as a privileged direction for regularization (Pierrot-Deseilligny, 2013).

A great advantage of MicMac is that it is open-source, which means that users may adapt it to their specific problems and also be involved improving the software.

2.3. Preliminary tests

A series of preliminary tests were performed on satellite images. First tests were carried out on images containing a synthetic sub-pixel deformation field, in order to test the capability of the correlators to retrieve this kind of deformation and evaluate their performances in the ideal case, where the deformation is perfectly known. First, we used images without diachronism, where the slave image was created by applying synthetic sub-pixel deformation on the master image (an example of images containing synthetic sub-pixel deformation is presented in Fig. 2 and the correlation results obtained with the three correlators on these images are in Figs. 3 and 4).

These tests allowed us to evaluate the three correlators’ parameters and do first comparisons between the correlators’ results and the theoretical displacement field. Second, tests were performed on two diachronic images, in order to test the influence of diachronism on the correlation results. In the diachronous case, we used two satellite ortho-images from the same place acquired several months apart, with no *a priori* deformation. The synthetic sub-pixel deformation (for a fault offset) was generated with Coulomb³ (a MATLAB add-on used by the geoscience community for seismotectonic simulations). This deformation was applied to the most recent image. Using synthetic diachronic images gives the opportunity of working on realistic scenario with the advantage of control over the amplitude and localization of the deformation. We found that the precision of the correlators on synthetic images is around 1/100 px on non-diachronic synthetic images and 1/10 px on diachronic ones.

Tests on the size of the correlation window have shown that MicMac, unlike the frequency-domain correlators, allows the use of a small correlation window without degrading the results, as it uses a regularization algorithm. For the frequency-domain correlators, the correlation noise increases significantly with decreasing size of the correlation window (Binet and Bollinger, 2005). According to Leprince et al., 2007b and Ayoub et al., 2009,

³ <http://www.coulombstress.org>.

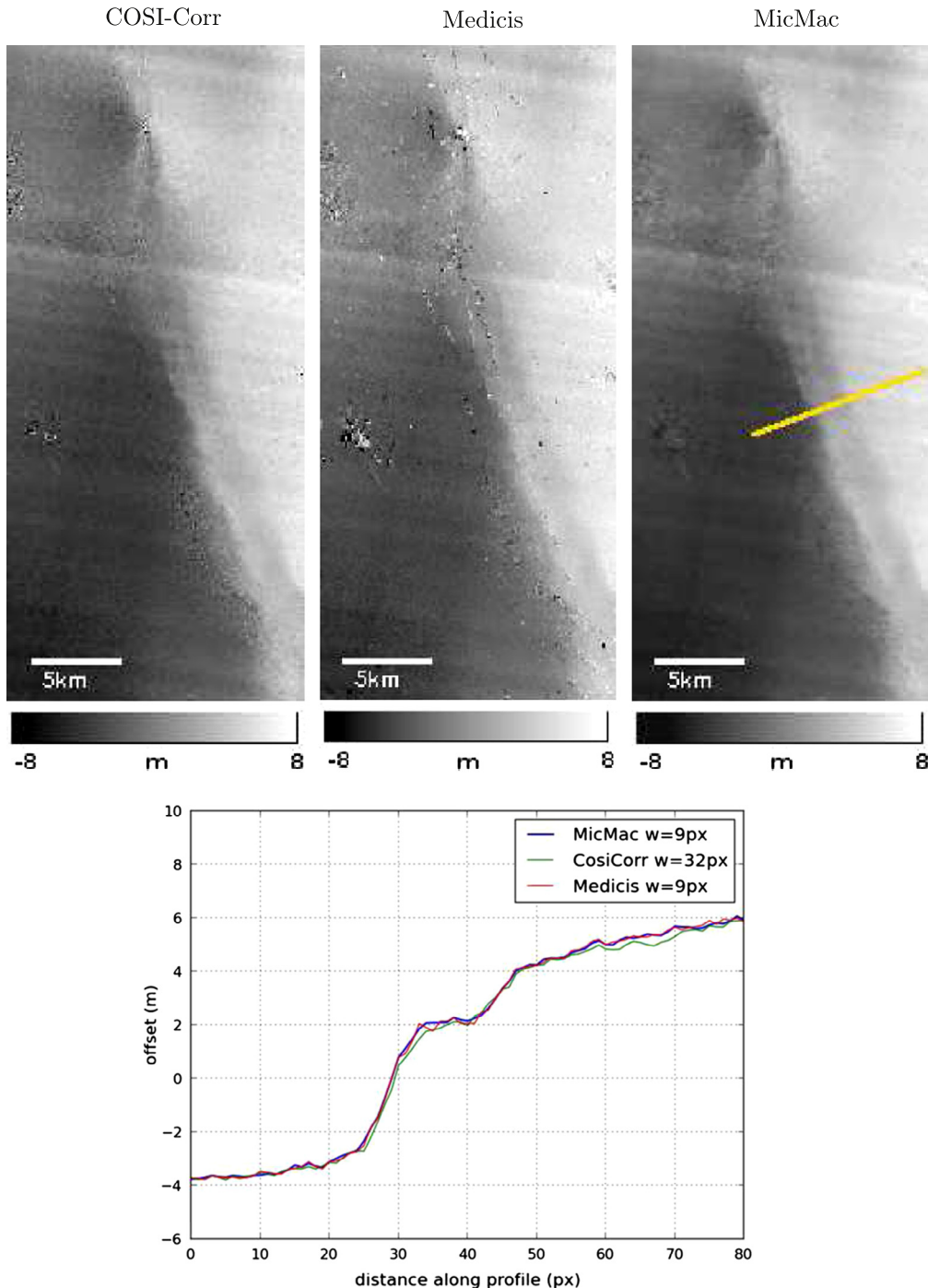


Fig. 8. East-west component of the offset field from the 2005 Afar dyke intrusion, using the pair of SPOT ortho-images from Fig. 7. The sizes of the correlation window used are 32×32 px for COSI-Corr and 9×9 px for Medicis and MicMac. Profiles are stacked over a width of 2.6 km and a length of 10.3 km using the weighted median method. All the three correlators detect two displacements corresponding to extension of ~ 7 m on the east-west axis.

for a frequency-domain correlator such as COSI-Corr, 32×32 px is considered a small window size. Therefore, testing it with what we consider to be a small correlation window (8×8 px) is an extreme case for this correlator, and less reliable results are to be expected. Thanks to MicMac's parametrization flexibility, we were able to test a pyramidal approach by incrementally decreasing the correlation window size. The results obtained in areas which correlate well are comparable to those obtained using the regularization method, but they rapidly degrade in difficult areas, with a greatly increased computation time.

3. Correlation results on real-case applications

In this paper we present the correlation results using the three correlators (MicMac, COSI-Corr and Medicis) on two co-seismic cases (instantaneous ground displacements due to the earthquake) and a dyke intrusion case (a rather slow event, which took place over ~ 20 days). For each case, we use two ortho-images bracketing the event. Real cases are of course more challenging, especially if there is a large interval of time between the two acquisition dates of the images which implies important changes, and therefore an

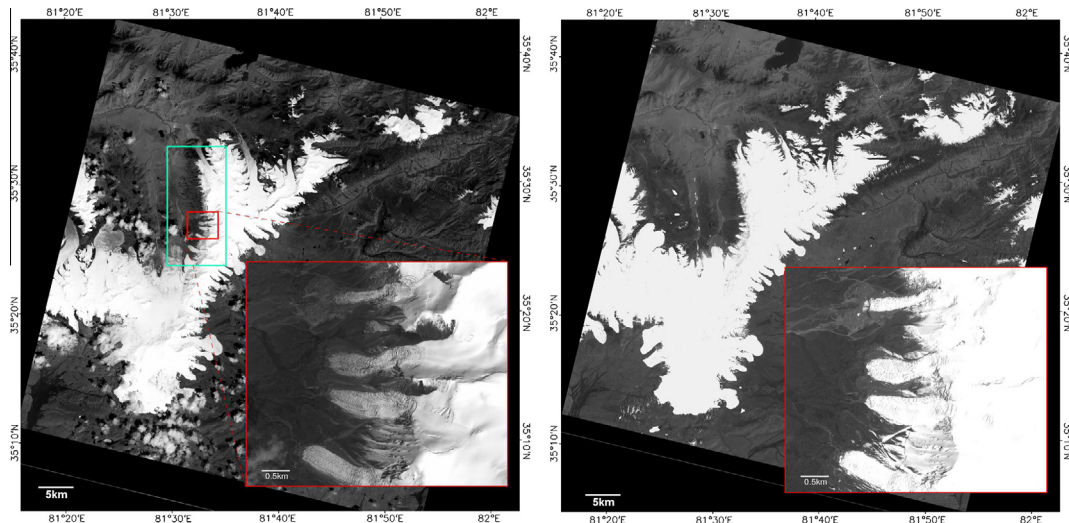


Fig. 9. The pair of ortho-images used for the study of the 2008 Yutian earthquake. Both the pre-event image (25 August 2002, incidence angle: L1.733520°) and the post-event one (26 June 2008, incidence angle: L2.206474°) are SPOT5 images. The fault is in an area covered almost entirely by the snow; surface ruptures are faintly visible across the glaciers in the after-event image (inset). The green box indicates the area where the results are presented in Figs. 10 and 11. (For interpretation of the references to color in this figure legend, the reader is referred to the web version of this article.)

increased risk of decorrelation. In all cases, the ground displacements were calculated from sub-pixel correlation of ortho-rectified SPOT panchromatic images. The topographic signal was removed from the optical images using the 3-arc-second SRTM digital elevation model.

In order to quantify the displacement, we developed FDSC (Fault Displacement Slip-Curve), a free, open-source program distributed under the CECILL-B license and available in the MicMac package.⁴ FDSC computes profiles perpendicular to the fault and then stacks them using the weighted median method, with the correlation scores as weights.

The correlation parameters for COSI-Corr, Medicis and MicMac valid for all three study cases are summarized in Table 1. The parameters are specific to each correlator. For MicMac, all the parameter values, including the correlation window size (9×9 px), were the same in all cases. For the two other correlators, it was necessary to adapt the correlation window size according to the noise level of the images. We tested many sizes of correlation windows. The choice of the window size is rather qualitative; for every correlator we present results from the smallest correlation window size which gave the clearest results.

3.1. The 2001 Kokoxili earthquake

The Kokoxili earthquake (moment magnitude $M_w \sim 7.8$, 14 November 2001) ruptured the Kunlun fault on the northern Tibetan Plateau over a total distance of ~ 450 km. It is one of the largest continental strike-slip earthquakes ever recorded (Klinger et al., 2005). In the case of a strike-slip fault, the fault surface is nearly vertical and the displacement is mainly horizontal. In Klinger et al., 2005; Klinger et al., 2006 the displacements on the Kunlun fault after the 2001 earthquake were estimated to ~ 4 m on average, with a maximum of 10 m.

We study the co-seismic displacements on a small section of this fault using the sub-pixel correlation on a SPOT1 pre-event image and a SPOT4 post-event image, with 10 m pixel size (Fig. 5). It is important to note the long temporal baseline (more than 13 years) between the two images.

On the section of the fault covered by our images, the horizontal displacement is considered to be fairly constant with an average displacement of ~ 3.5 m and a maximum of $\sim 4.5\text{--}5$ m (Xu et al., 2006).

The correlation was performed with the three correlators using small and large correlation windows. The use of small correlation windows is important in order to preserve the signal.

For all three correlators, no significant discontinuity is detectable in the north-south component of the co-seismic offset field. The deformation is detected only in the east-west component of the correlation.

In the case of large correlation windows, the correlation was calculated on a 64×64 px window (for COSI-Corr) and a 65×65 px window (for Medicis) with a step of 16 px yielding a ground pixel size of 160 m. For MicMac, the correlation window size was 65×65 px. The sizes of the small correlation windows were 8×8 px (for COSI-Corr) and 9×9 px (for Medicis) with a step of 4 px (yielding a ground pixel size of 40 m), and 9×9 px for MicMac. The MicMac results are in full resolution; therefore they are downsampled in order to have a pixel size comparable to the other two correlators.

For the small correlation window, COSI-Corr's result is very noisy and the amplitude of the co-seismic offset is underestimated (Fig. 6). MicMac gives good results in terms of noise and amplitude of the deformation retrieved from the stacks of profiles perpendicular to the fault. The results of Medicis are a bit noisy, but the amplitude of the offset corresponds to the amplitude retrieved by MicMac.

For the large correlation window, all three correlators retrieve the same amplitude of deformation (~ 4.5 m, consistent to the displacements measured by Xu et al. (2006), Klinger et al. (2005), Klinger et al. (2006)). The results of Medicis and MicMac are more blurry than when using small correlation windows.

Therefore, for the other studies, we present the COSI-Corr's results for correlation windows with a minimum size of 32×32 px (Leprince et al., 2007b). For Medicis we present the results either for the small correlation window (when possible, if the correlation noise permits it) or the large one (a window size equivalent to the one used for COSI-Corr). All results for MicMac are for the small correlation window (9×9 px). For the sake of consistency, all the correlators' results presented were downsampled by a factor equal to the step used for the COSI-Corr correlation.

⁴ http://logiciels.ign.fr/?Telechargement_20.

3.2. The 2005 dyke intrusion in Afar

Between 2005 and 2010, a rifting episode with 14 dyke intrusions occurred in the Manda-Hararo rift in Afar (Ethiopia). The first and largest dyke intruded on 26 September 2005 and ruptured the entire 60-kilometer-long rift segment (Yirgu et al., 2006; Ayele et al., 2007; Grandin et al., 2009), opening the rift with a maximum extension of about 6 m (Ayele et al., 2007; Grandin et al., 2009; Barisin et al., 2009). Such rifting events include tectonic and magmatic processes which lead to the separation of two divergent tectonic plates. In the case of a dyke intrusion, most of the deformation is aseismic (or “silent”), so the seismic energy (quantified by the moment magnitude scale M_w) is less relevant, but an

equivalent moment magnitude (M_{eq}) of ~ 7.0 is computed based on inversion of geodetic data and the geometry of the dyke (Grandin et al., 2009). The September 2005 event is considered to be the largest rifting episode ever observed on land (Yirgu et al., 2006).

In order to measure the horizontal displacements induced by this intrusion, correlation was performed on two 8 m-resolution SPOT4 ortho-images separated by 13 months (Fig. 7). The correlation window size selected for COSI-Corr was 32×32 px with a 16 px step, yielding a ground pixel size of 128 m. For Medicis and MicMac, the correlation window used was 9×9 px and their results were downsampled by a factor equal to the COSI-Corr step. The east-west results (Fig. 8) show that the three correlators detect two displacements corresponding to extension of the rift by a total

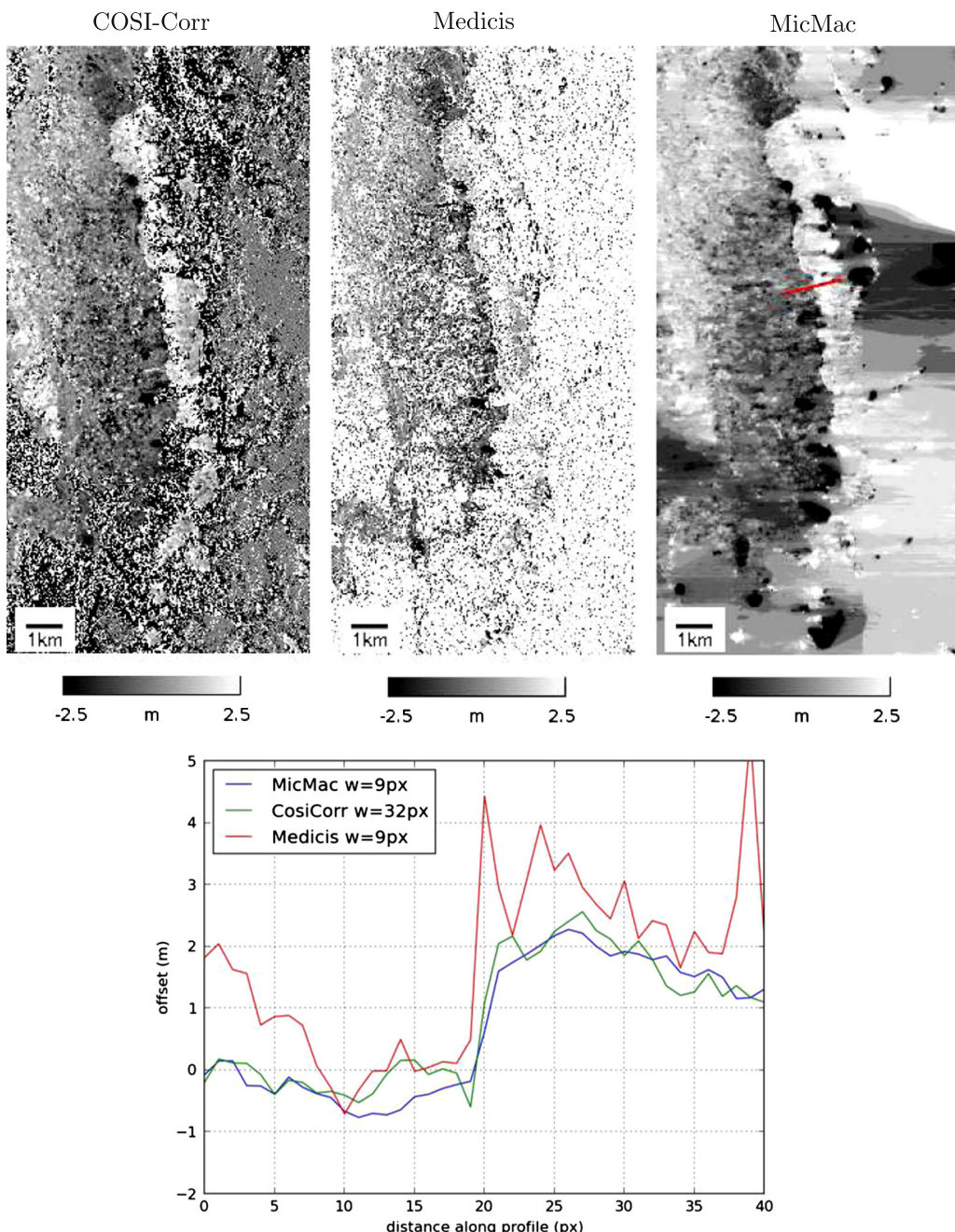


Fig. 10. East-west component of the co-seismic offset field from the 2008 Yutian earthquake, using the pair of SPOT ortho-images from Fig. 9. The sizes of the correlation windows used are 32×32 px for COSI-Corr, 9×9 px for Medicis and 9×9 px for MicMac. Profiles are stacked over a width of 1.6 km and a length of 1.6 km using the weighted median method. COSI-Corr (with a large correlation window) and MicMac (with a small correlation window) retrieve both a co-seismic offset of ~ 2.7 m; Medicis' results for a small correlation window are not satisfactory, the amplitude of the offset is not well retrieved.

of ~ 7 m. All three correlators detect the same amplitude of displacement, which exceeds the ~ 6 m maximum extension value from (Grandin et al., 2009; Barisin et al., 2009; Ayele et al., 2007). This discrepancy seems to be caused by a problem in the ortho-images, independent of the correlation, most likely due to inaccuracies in the determination of the satellite attitude (Grandin et al., 2009) and distortions induced by charge-coupled device (CCD) misalignments (Barisin et al., 2009).

3.3. The 2008 Yutian earthquake

The Yutian earthquake ($M_w \sim 7.1$, 21 March 2008) on the Tibetan Plateau is one of the largest recent continental normal fault earthquakes (Elliott et al., 2010). Normal faults develop in areas of

extension and the movement on the fault includes both vertical and horizontal displacement. The co-seismic horizontal displacement is measured using correlation of two 5 m-resolution SPOT5 ortho-images (Fig. 9). In addition to a time interval of nearly 6 years between the two images, snow covers large percentage of the images (including the fault area) which makes the correlation extremely difficult to compute. The surface deformation associated with this earthquake is primarily in the east-west direction (Elliott et al., 2010), so it is retrieved by the east-west correlation map (Fig. 10 and Fig. 11). The maximum horizontal offset measured in the field by Xu et al. (2013) is ~ 3.6 m.

In this case, for COSI-Corr the best results were obtained with a correlation window of 32×32 px with a 8 px step, yielding a ground pixel size of 40 m. For Medicis, as the results obtained

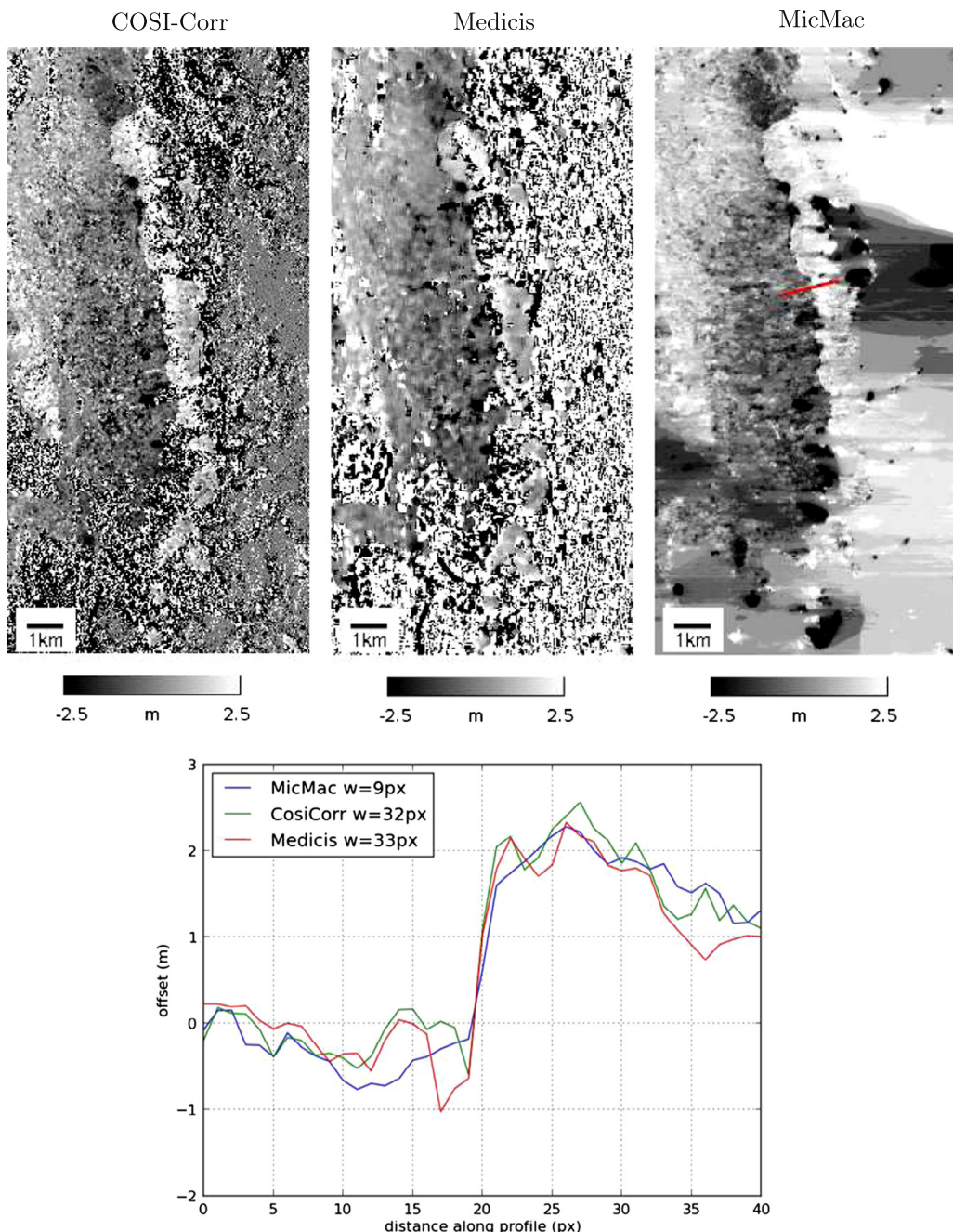


Fig. 11. East-west component of the co-seismic offset field from the 2008 Yutian earthquake, using the pair of SPOT ortho-images from Fig. 9. The sizes of the correlation windows used are 32×32 px for COSI-Corr, 33×33 px for Medicis and 9×9 px for MicMac. Profiles are stacked over a width of 1.6 km and a length of 1.6 km using the weighted median method. All three correlators retrieve a co-seismic offset of ~ 2.7 m.

using a small correlation window (9×9 px, Fig. 10) are not satisfactory, the results are then presented for a correlation window size comparable to the one used for COSI-Corr (Fig. 11). For this very difficult case, MicMac proves to be the only correlator capable of using a small correlation window and it also offers a clearer image of the fault offset. In Fig. 11, the amplitudes of displacement retrieved by MicMac (correlation window size 9×9 px), COSI-Corr (32×32 px) and Medicis (33×33 px) are ~ 2.7 m. This value is in agreement with Xu et al. (2013).

4. Discussion/conclusion

Numerous tests have been carried out to determine the best parameters for the three correlators and the results selected were the best ones for each correlator. Unlike MicMac and Medicis, COSI-Corr does not have many parameters for the user to choose, which can be seen as an advantage (it is very easy to use), but also as a drawback as the user does not have a lot of options especially for difficult correlation cases. Medicis is fairly easy to use despite the high number of parameters and no graphical user interface. MicMac also has a large number of parameters but a simple command line interface, dedicated to measuring ground displacements, is available (Pierrot-Deseilligny, 2013).

Our suite of examples allowed us to evaluate the performance of each correlator. For the Kokoxili earthquake, the primary challenges were the long temporal baseline between the two SPOT1 and SPOT4 images used, the highly mountainous snowy area of the fault, and the use of multi-sensor images. It allowed us to study how each correlator managed to find the fault signal in a difficult case, testing small and large correlation windows. Our main interest is to have very detailed results in order to finely evaluate the ground deformation, therefore using small correlation windows is essential if the correlation noise allows it. The Afar dyke intrusion was a favorable study case in terms of imaging conditions: it occurred in a desertic area with no significant seasonal variations, and the time interval between the two SPOT4 images was relatively short. The Yutian earthquake was an especially difficult case: the relatively long temporal baseline of almost 6 years between the two SPOT5 images and the snow made it extremely difficult if not impossible to retrieve the fault signal due to the high risk of decorrelation. Due to all these unfavorable conditions, this was an extreme test of the correlators' efficiency.

As expected for a frequency-domain correlator, COSI-Corr gave very good results when using large correlation windows (minimum 32×32 px, as specified in Leprince et al. (2007b) and Ayoub et al. (2009)), but not satisfactory results when using smaller correlation windows. However, despite using the frequency domain, Medicis retrieved accurate deformation amplitudes for the first and second study cases using a small correlation window. For the most difficult (Yutian) study case, MicMac was the only correlator capable of giving good results at small correlation window and it offered a better picture of the fault signal. Thanks to its features (e.g. regularization, non-linear correlation cost), MicMac appears to be less vulnerable to noise and to be able to deal with large spatial inhomogeneities due to long time intervals, snow and seasonal changes. MicMac proves to be a quality free open-source alternative for image correlation for ground deformation measurements.

Acknowledgements

The authors would like to thank CNES for funding this project through the TOSCA program and for kindly lending us Medicis. We thank Stéphane May for his valuable help with Medicis, and Raphaël Grandin, Stéphanie Dumont and Belle Philibosian for their

constructive comments. We are grateful to two anonymous reviewers that helped to improve this manuscript. This is IPGP contribution number 3501.

References

- Ayele, A., Jacques, E., Kassim, M., Kidane, T., Omar, A., Tait, S., Nercessian, A., de Chabalier, J.-B., King, G., 2007. The volcano-seismic crisis in Afar, Ethiopia, starting September 2005. *Earth Planetary Sci. Lett.* 255, 177–187. <http://dx.doi.org/10.1016/j.epsl.2006.12.014>.
- Ayoub, F., Leprince, S., Keene, L., 2009. User's Guide to COSI-CORR, Co-registration of Optically Sensed Images and Correlation. <http://tectonics.caltech.edu/slip_history/spot_coseis>.
- Barisin, I., Leprince, S., Parsons, B., Wright, T., 2009. Surface displacements in the September 2005 Afar rifting event from satellite image matching: asymmetric uplift and faulting. *Geophys. Res. Lett.* 36 (L07301). <http://dx.doi.org/10.1029/2008GL036431>.
- Bicheron, P., Amberg, V., Bourg, L., Petit, D., Huc, M., Miras, B., Brockmann, C., Delwart, S., Ranéra, F., Hagolle, O., Leroy, M., Arino, O., 2011. Geolocation assessment of MERIS GlobCover orthorectified products. *IEEE Trans. Geosci. Remote Sens.* 49 (8), 2972–2982. <http://dx.doi.org/10.1109/TGRS.2011.2122337>.
- Binet, R., Bollinger, L., 2005. Horizontal coseismic deformation of the 2003 Bam (Iran) earthquake measured from SPOT-5 THR satellite imagery. *Geophys. Res. Lett.* 32 (L02307). <http://dx.doi.org/10.1029/2004GL021897>.
- Casson, B., Delacourt, C., Allemand, P., 2005. Contribution of multi-temporal remote sensing images to characterize landslide slip surface – application to the La Clapière landslide (France). *Nat. Hazards Earth Syst. Sci.* (5), 425–437.
- Delacourt, C., Allemand, P., Casson, B., Vadon, H., 2004. Velocity field of the "La Clapière" landslide measured by the correlation of aerial and QuickBird satellite images. *Geophys. Res. Lett.* 31 (L15619). <http://dx.doi.org/10.1029/2004GL020193>.
- Dominguez, S., Avouac, J.-P., Michel, R., 2003. Horizontal coseismic deformation of the 1999 Chi-Chi earthquake measured from SPOT satellite images: implications for the seismic cycle along the western foothills of central Taiwan. *J. Geophys. Res.* 108 (B2). <http://dx.doi.org/10.1029/2001JB000951>.
- Elliott, J.R., Walters, R.J., England, P.C., Jackson, J.A., Li, Z., Parsons, B., 2010. Extension on the Tibetan plateau: recent normal faulting measured by InSAR and body wave seismology. *Geophys. J. Int.* (183), 503–535. <http://dx.doi.org/10.1111/j.1365-246X.2010.04754.x>.
- Grandin, R., Socquet, A., Binet, R., Klinger, Y., Jacques, E., de Chabalier, J.-B., King, G.C.P., Lasserre, C., Tait, S., Tapponnier, P., Delorme, A., Pinzuti, P., 2009. September 2005 Manda Hararo-Dabbahu rifting event, Afar (Ethiopia): constraints provided by geodetic data. *J. Geophys. Res.* 114 (B08404). <http://dx.doi.org/10.1029/2008JB005843>.
- Guérin, C., Binet, R., Pierrot-Deseilligny, M., 2012. Détection des changements d'élévation d'une scène par imagerie satellite stéréoscopique. In: Reconnaissance des Formes et Intelligence Artificielle (RFIA), Lyon, France.
- Hermas, E., Leprince, S., El-Magd, I.A., 2012. Retrieving sand dune movements using sub-pixel correlation of multi-temporal optical remote sensing imagery, northwest Sinai Peninsula, Egypt. *Remote Sens. Environ.* 121, 51–60. <http://dx.doi.org/10.1016/j.rse.2012.01.002>.
- Hollingsworth, J., Leprince, S., Ayoub, F., Avouac, J.-P., 2012. Deformation during the 1975–1984 Krafla rifting crisis, NE Iceland, measured from historical optical imagery. *J. Geophys. Res.* 117 (B11407). <http://dx.doi.org/10.1029/2012JB009140>.
- Inglada, J., Muron, V., Pichard, D., Feuvrier, T., 2007. Analysis of artifacts in subpixel remote sensing image registration. *IEEE Trans. Geosci. Remote Sens.* 45 (1), 254–264. <http://dx.doi.org/10.1109/TGRS.2006.882262>.
- Klinger, Y., Xu, X., Tapponnier, P., der Woerd, J.V., Lasserre, C., King, G., 2005. High-resolution satellite imagery mapping of the surface rupture and slip distribution of the $M_w \sim 7.8$, 14 November 2001 Kokoxili Earthquake, Kunlun Fault, Northern Tibet, China. *Bull. Seismol. Soc. Am.* 95 (5), 1970–1987. <http://dx.doi.org/10.1785/0120040233>.
- Klinger, Y., Michel, R., King, G., 2006. Evidence for an earthquake barrier model from $M_w \sim 7.8$ Kokoxili (Tibet) earthquake slip-distribution. *Earth Planet. Sci. Lett.* (242), 354–364. <http://dx.doi.org/10.1016/j.epsl.2005.12.003>.
- Leprince, S., Ayoub, F., Klinger, Y., Avouac, J.-P., 2007a. Co-registration of optically sensed images and correlation (COSI-Corr): an operational methodology for ground deformation measurements, in: IEEE International Geoscience and Remote Sensing Symposium (IGARSS), Barcelona, Spain.
- Leprince, S., Barbot, S., Ayoub, F., Avouac, J.-P., 2007b. Automatic and precise orthorectification, coregistration, and subpixel correlation of satellite images, application to ground deformation measurements. *IEEE Trans. Geosci. Remote Sens.* 45 (6), 1529–1558. <http://dx.doi.org/10.1109/TGRS.2006.888937>.
- Lisein, J., Pierrot-Deseilligny, M., Bonnet, S., Lejeune, P., 2013. A photogrammetric workflow for the creation of a forest canopy height model from small unmanned aerial system imagery. *Forests* 4 (4), 922–944. <http://dx.doi.org/10.3390/f4040922>.
- Massonnet, D., Feigl, K.L., 1998. Radar interferometry and its application to changes in the Earth's surface. *Rev. Geophys.* 36 (4), 441–500.
- Michel, R., Avouac, J.-P., 2002. Deformation due to the 17 August 1999 Izmit, Turkey, earthquake measured from SPOT images. *J. Geophys. Res.* 107. <http://dx.doi.org/10.1029/2000JB000102>.

- Pierrot-Deseilligny, M., 2013. MicMac, Apero, Pastis and Other Beverages in a Nutshell. <<http://logiciels.ign.fr/?Micmac>>.
- Pierrot-Deseilligny, M., Paparoditis, N., 2006. A multiresolution and optimization-based image matching approach: an application to surface reconstruction from SPOT5-HRS stereo imagery. In: ISPRS Workshop on Topographic Mapping from Space (With Special Emphasis on Small Satellites), Ankara, Turkey.
- Scambos, T.A., Dutkiewicz, M.J., Wilson, J.C., Bindschadler, R.A., 1992. Application of image cross-correlation to the measurement of glacier velocity using satellite image data. *Remote Sens. Environ.* 42 (3), 177–186.
- Thévenaz, P., Blu, T., Unser, M., 2000. Interpolation revisited. *IEEE Trans. Med. Imag.* 19 (7), 739–758.
- Van Puymbroeck, N., Michel, R., Binet, R., Avouac, J.-P., Taboury, J., 2000. Measuring earthquakes from optical satellite images. *Appl. Opt.* 39 (20), 3486–3494.
- Xu, X., Yu, G., Klinger, Y., Tapponniere, P., Van Der Woerd, J., 2006. Reevaluation of surface rupture parameters and faulting segmentation of the 2001 Kunlunshan earthquake (M_w 7.8), northern Tibetan Plateau, China. *J. Geophys. Res.* 111 (B05316). <http://dx.doi.org/10.1029/2004JB003488>.
- Xu, X., Tan, X., Yu, G., Wu, G., Fang, W., Chen, J., Song, H., Shen, J., 2013. Normal- and oblique-slip of the 2008 Yutian earthquake: evidence for eastward block motion, northern Tibetan Plateau. *Tectonophysics* 584, 152–165. <http://dx.doi.org/10.1016/j.tecto.2012.08.007>.
- Yirgu, G., Ayele, A., Ayalew, D., 2006. Recent seismovolcanic crisis in Northern Afar, Ethiopia. *EOS* 87 (33), 325–329.